The Plant Cell, Vol. 17, 705–721, March 2005, www.plantcell.org

The Arabidopsis *GAMYB-Like* Genes, *MYB33* and *MYB65*, Are MicroRNA-Regulated Genes That Redundantly Facilitate Anther Development

Anthony A. Millar[a,b,1] and Frank Gubler[a]

[a] Commonwealth Scientific and Industrial Research Organization, Division of Plant Industry, Canberra ACT 2601, Australia
[b] Graingene, Griffith ACT 2603, Australia

The functions of the vast majority of genes encoding R2R3 MYB domain proteins remain unknown. The closely related *MYB33* and *MYB65* genes of *Arabidopsis thaliana* have high sequence similarity to the barley (*Hordeum vulgare*) *GAMYB* gene. T-DNA insertional mutants were isolated for both genes, and a *myb33 myb65* double mutant was defective in anther development. In *myb33 myb65* anthers, the tapetum undergoes hypertrophy at the pollen mother cell stage, resulting in premeiotic abortion of pollen development. However, *myb33 myb65* sterility was conditional, where fertility increased both under higher light or lower temperature conditions. Thus, *MYB33*/*MYB65* facilitate, but are not essential for, anther development. Neither single mutant displayed a phenotype, implying that *MYB33* and *MYB65* are functionally redundant. Consistent with functional redundancy, promoter–β-glucuronidase (GUS) fusions of *MYB33* and *MYB65* gave identical expression patterns in flowers (sepals, style, receptacle, anther filaments, and connective but not in anthers themselves), shoot apices, and root tips. By contrast, expression of a *MYB33*:GUS translational fusion in flowers was solely in young anthers (consistent with the male sterile phenotype), and no staining was seen in shoot meristems or root tips. A microRNA target sequence is present in the *MYB* genes, and mutating this sequence in the *MYB33*:GUS fusion results in an expanded expression pattern, in tissues similar to that observed in the promoter-GUS lines, implying that the microRNA target sequence is restricting *MYB33* expression. Arabidopsis transformed with *MYB33* containing the mutated microRNA target had dramatic pleiotrophic developmental defects, suggesting that restricting *MYB33* expression, especially in the shoot apices, is essential for proper plant development.

INTRODUCTION

With >120 genes in the *Arabidopsis thaliana* genome, the *R2R3-MYB* gene family has been identified as one of the most abundant classes of transcription factors in plants (Stracke et al., 2001). They are involved in a diverse range of processes, including controlling cell shape, disease resistance, regulating secondary metabolism, and hormone signal transduction (Jin and Martin, 1999). One *MYB* gene from barley (*Hordeum vulgare*), *HvGAMYB*, is involved in gibberellin (GA) signaling in the aleurone (Gubler et al., 1995). Here, expression of HvGAMYB is upregulated by GA, where it then binds to the TAACAAA motif of a barley high-pI α-amylase promoter, a motif that plays an important role in the GA-regulated expression of the α-amylase gene (Skriver et al., 1991; Gubler and Jacobsen, 1992; Lanahan et al., 1992). In transient assays, constitutive expression of HvGAMYB is sufficient to activate the α-amylase promoter (Gubler et al., 1995) and the promoters of other aleurone GA-regulated genes that are required for the mobilization of endosperm reserves (Cercós et al., 1999; Gubler et al., 1999). Thus, in regards to expression of these genes in aleurone layers, transient expression of *HvGAMYB* has the same effect as GA application. From this, it has been concluded that HvGAMYB is a positive regulator of the GA signal transduction pathway in the barley aleurone.

Recently, several studies have examined the role of GAMYB outside the aleurone. In rice (*Oryza sativa*), three independent *Tos17* insertion alleles in the *GAMYB* gene have been isolated (Kaneko et al., 2004). As predicted, no α-amylase expression was induced in *gamyb* seeds that had been treated with GA, confirming the role of *GAMYB* in induction of α-amylase expression. Although no vegetative phenotype was observed in *gamyb* plants, after phase transition to the reproductive stage, shortened internodes and defects in floral organs were observed, especially defects in anthers (Kaneko et al., 2004). These phenotypic deviations from wild-type plants were consistent with the pattern of expression of the *GAMYB* gene. Similar results were found in barley, where *HvGAMYB* was found to be strongly expressed in the anthers, and transgenic barley overexpressing *HvGAMYB* was male sterile (Murray et al., 2003). However, whereas the male sterility in barley was due to the failure of anthers to dehisce, the block in the rice *gamyb* plants occurred before meiosis. Other studies have implicated a role for

[1] To whom correspondence should be addressed. E-mail tony.millar@csiro.au; fax 61-2-62465270.
The author responsible for distribution of materials integral to the findings presented in this article in accordance with the policy described in the Instructions for Authors (www.plantcell.org) is: Anthony A. Millar (tony.millar@csiro.au).
Article, publication date, and citation information can be found at www.plantcell.org/cgi/doi/10.1105/tpc.104.027920.

GAMYB in endosperm development in barley (Diaz et al., 2002), elongation of the first internode in wheat (*Triticum aestivum*) (Chen et al., 2001), and flowering in *Lolium temulentum* (Gocal et al., 1999).

In Arabidopsis, there is a small family of *GAMYB-like* genes (Gocal et al., 2001). Construction of a phylogenetic tree with the entire *MYB* gene family of Arabidopsis groups five genes (*MYB33*, *MYB65*, *MYB97*, *MYB101*, and *MYB120*) with *HvGAMYB* (Stracke et al., 2001). Furthermore, these five genes contain a unique intron located at the 3′ end of the open reading frame, implying that they belong to a distinct subclass in the MYB superfamily of transcription factors. Previously, *MYB33*, *MYB65*, and *MYB101* have been shown to be able to substitute for *HvGAMYB* in transactivating the α-amylase promoter in barley aleurone layer assays (Gocal et al., 2001). The expression of these genes was consistent with roles in GA-mediated processes, with expression of *MYB33* at the shoot apex coinciding with the onset of flowering, either when endogenous GA levels increased or when GA was applied to the plants (Gocal et al., 2001).

Recent evidence suggests that the *GAMYB-like* genes are subjected to posttranscriptional regulation by microRNAs (miRNAs). Initially, three Arabidopsis miRNAs, miR159a, b, and c, were identified that have complementarity to a highly conserved motif in the coding region of the *GAMYB-like* genes (Park et al., 2002; Rhoades et al., 2002). The isolation of miRNA-guided cleavage products for both the *MYB33* and *MYB65* genes further suggests these genes are being regulated by miRNAs (Palatnik et al., 2003), and using an *Agrobacterium tumefaciens*–mediated delivery system, it has been shown that miR159a can cleave *MYB33* mRNA in planta (Achard et al., 2004). Furthermore, Arabidopsis plants with mutations in genes involved in miRNA-mediated gene regulation, such as *hua enhancer 1* or *hyponastic leaves 1*, have much higher steady state levels of *MYB33* transcripts when compared with wild-type plants (Han et al., 2004), whereas plants overexpressing miR159a have decreased levels of *MYB33*, are male sterile, and have delayed flowering time (Achard et al., 2004). Finally, this miRNA target motif has been shown to be functionally important, for 35S expression of a *MYB33* gene with a mutated miRNA target sequence (*mMYB33*) results in plants with an altered leaf morphology, which is in contrast with 35S expression of a wild-type *MYB33* gene that results in no observable phenotype (Palatnik et al., 2003).

In this article, we describe T-DNA–tagged mutants in two of the Arabidopsis *GAMYB-like* genes, *MYB33* and *MYB65*, and show that these genes act redundantly in anther development. Using a series of β-glucuronidase (GUS) reporter constructs, we demonstrate that the miR159 target motif restricts *MYB33* expression, and when this motif is absent, aberrant *MYB33* gene expression occurs, resulting in gross defects in plant growth and development.

RESULTS

The Duplicated Genes *MYB33* and *MYB65* Are Putative *GAMYB* Orthologs

Based on several different phylogenetic trees, *MYB33* and *MYB65* are the Arabidopsis genes with the highest similarity to the *GAMYB* genes of cereals (Stracke et al., 2001; Yang et al., 2001). Furthermore, MYB33 and MYB65 have high sequence similarity to one another. Overall, they are 58.4% identical at the amino acid level, with >90% identity shared between their R2R3 domains but only 51.0% identity in their C-terminal domains. Analysis of their chromosomal locations reveal that they lie within segmental duplicated regions of the Arabidopsis genome (Arabidopsis Genome Initiative, 2000), for the genes immediately upstream of the *MYB* genes encode proteins that have high sequence identity with one another (81.2% amino acid identity) as do the genes immediately downstream (69.7% amino acid identity). In addition to being duplicated genes, Gocal et al. (2001) found that they have similar expression patterns. These two facts make them strong candidates for being functionally redundant in the plant.

Isolation and Characterization of T-DNA Insertional Mutants in the *MYB33* and *MYB65* Genes

To determine the function of the Arabidopsis *GAMYB-like* genes, we undertook a reverse genetic approach and isolated T-DNA mutant alleles for both *MYB33* and *MYB65*. Using a PCR-based screen on populations of T-DNA tagged lines, we identified one mutant that contained a T-DNA insert in the region encoding the R2R3 domain of the *MYB33* gene, 15 amino acids into the R3 domain (Figure 1A). This insertion is likely to result in a null allele of *MYB33* and was designated *myb33*. To help determine the number of T-DNA inserts, we performed DNA gel blot analysis on DNA from homozygous *myb33* plants using the *uidA* (GUS) gene as a probe. Each lane had two to three hybridizing bands (data not shown), indicating that multiple T-DNA copies are present in the *myb33* mutant line. In addition, segregation analysis for the *nptII* gene was performed by selecting for growth on medium containing kanamycin (50 μg/mL) with seeds from a heterozygous *myb33* plant. There were 203 resistant plants and 76 sensitive plants that approximates to a 3:1 ratio ($\chi^2 = 0.746$; $P > 0.25$), implying that the T-DNAs segregated as one locus. This suggests that either multiple T-DNAs have inserted into one site as a concatamer, or T-DNAs have inserted into multiple linked sites. Plants homozygous for the *myb33* allele were isolated; however, there were no obvious morphological alterations to the plants.

One mutant was found in which a T-DNA had inserted into the coding region of the *MYB65* gene. In this allele, designated *myb65*, the T-DNA had inserted into the region of the gene that encodes Box 1 (Gocal et al., 2001), a conserved motif amongst the *GAMYB-like* genes that is immediately C-terminal to the R2R3 domain (Figure 1B). Both T-DNA/plant junctions could be amplified with the left border primer, JL202, implying that tandem T-DNAs had inserted into this locus in an inverted fashion. Restriction fragment patterns of a genomic DNA gel blot of *myb65* hybridized to the GUS gene were consistent with this (data not shown). DNA digested with *Eco*RI gave a single expected band of 4.9 kb, whereas a *Hin*dIII digest gave two bands of >10 and 6.8 kb, which are consistent with the predicted restriction map (Figure 1B) and implying that there is only one T-DNA locus present in the plant. This is supported by segregation analysis of progeny of a *MYB65*/*myb65* heterozygote on

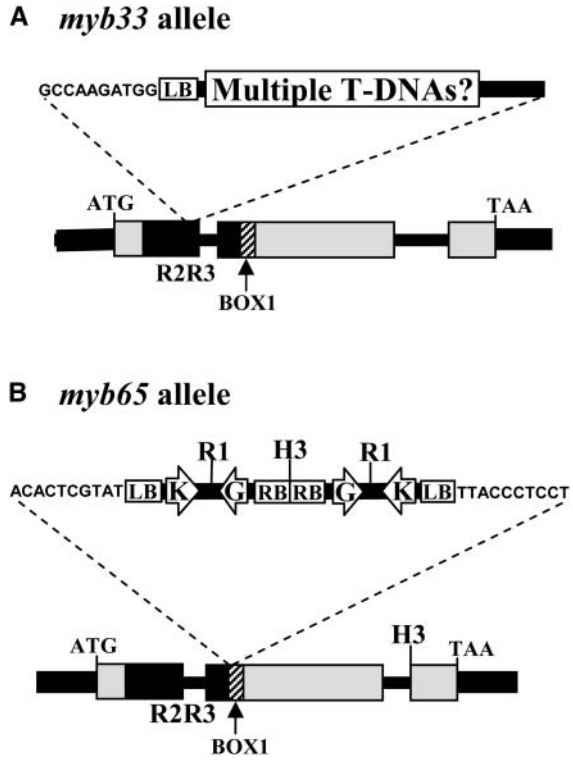

Figure 1. Structure of the T-DNA Insertional Mutants.

(A) Structure of the *myb33* allele.
(B) Structure of the *myb65* allele.
Arrows indicate the location of the *neomycin-phosphotransferase II* gene (K) and the *uidA* gene driven by the −60 35S *Cauliflower mosaic virus* promoter (G). LB, left border; RB, right border; R1, *Eco*RI; H3, *Hin*dIII. As determined by sequencing the T-DNA/plant DNA junctions, the 10 nucleotides of Arabidopsis DNA flanking the T-DNAs are shown.

growth medium containing kanamycin (50 μg/mL). Here, 425 resistant plants were obtained compared with 135 sensitive plants, again an approximate 3:1 ratio ($\chi^2 = 0.237$; $P > 0.5$). In addition to the T-DNA insertion, 20 bp of the wild-type gene had been deleted. Thus, like the *myb33* allele, it is assumed a nonfunctional protein is produced. Plants homozygous for the *myb65* allele were isolated; however, there was no visible phenotype in these plants.

Double Mutant *myb33 myb65* Plants Are Male Sterile

Although both single mutants have predicted loss-of-function alleles, neither *myb33* nor *myb65* plants show any detectable differences from wild-type plants. Thus, the generation of a *myb33 myb65* double mutant may be necessary to elucidate their function(s). A cross was made between homozygous *myb33* and homozygous *myb65* plants. Of 173 F2 plants, nine plants failed to set seed. Using both PCR genotyping and genomic DNA gel blot analysis, it was found that only these plants were *myb33 myb65* double mutants (data not shown). A 164:9 ratio is consistent with a 15:1 ratio ($\chi^2 = 0.323$; $P > 0.5$) expected with two segregating recessive loci. This implies that only plants homozygous for both *myb33* and *myb65* are sterile and that the presence of only one copy of *MYB33* or *MYB65* is enough to result in fertile plants.

Stamens of *myb33 myb65* were typically shorter than their wild-type counterparts (Figure 2A) and failed to fully extend to the pistil (Figure 2B). Furthermore, anthers from the mutant plants were smaller than the wild type and failed to produce pollen, indicating that the mutant is male sterile. Reciprocal crosses between *myb33 myb65* and wild-type plants demonstrated that the female parts of the *myb33 myb65* plant were fully fertile and confirmed the male sterile phenotype of *myb33 myb65*. Other than sterility and the associated characteristics of sterile plants, such as the increased numbers of flowers per inflorescence, *myb33 myb65* shows no obvious morphological differences from wild-type plants. These observations were on plants grown under continuous light at ~80 $\mu mol \cdot m^{-2} s^{-1}$ light intensity and 21°C.

Of the nine *myb33 myb65* plants obtained, two plants eventually set seed. From one plant, one silique was present, from which five seeds were obtained, and in the second plant, three consecutive siliques set seed, from which 44 seeds were obtained. PCR genotyping was performed on the F3 plants derived from these seed, and they were all shown to be *myb33 myb65* double mutants, implying that these seeds arose through a self-crossing event. Like their F2 parents, these F3 plants were also male sterile, but again would sporadically produce partially or completely filled siliques. Along the bolt, sterility could cycle, with filled siliques followed by a few empty siliques (unfertilized carpels) and then again more filled siliques (Figure 2C). The unusual characteristic of this mutant is that a plant may only produce several siliques containing seeds and that these siliques may contain close to the same number of seeds as siliques from a wild-type plant. Thus, occasionally during the plant's life it is able to produce pollen and set seed. This is different from the known reduced fertility mutants of Arabidopsis that have been classified as having consistently short siliques (Sanders et al., 1999). Thus, the *myb33 my65* double mutant appears to represent a new class of male sterile mutant in Arabidopsis.

Because of the presence of multiple T-DNAs in the *myb33* allele, molecular complementation was needed to confirm that the male sterile phenotype observed in *myb33 myb65* was in fact due to a mutant *MYB33* gene. A genomic clone of *MYB33* was transformed into *myb33 myb65*, and 25 of 30 T1 plants had fertility entirely restored. Fertile and sterile plants were found to be segregating in the progeny, and the transgene was found by PCR to be segregating with the fertile plants (data not shown), confirming that the *MYB33* gene is able to complement the male sterile phenotype. For *MYB65*, an additional allele was obtained from the SALK collection (SALK_063552), which we designated *myb65-2*. We constructed a *myb33 myb65-2* double mutant and found again the plants were male sterile. This second allele confirms that *MYB65* is required for proper anther development in Arabidopsis.

The Block in Pollen Development Occurs Premeiotically Where the Tapetum Undergoes Hypertrophy

Transverse sections of wild-type and double mutant Arabidopsis anthers were prepared and stained with toluidine blue to identify

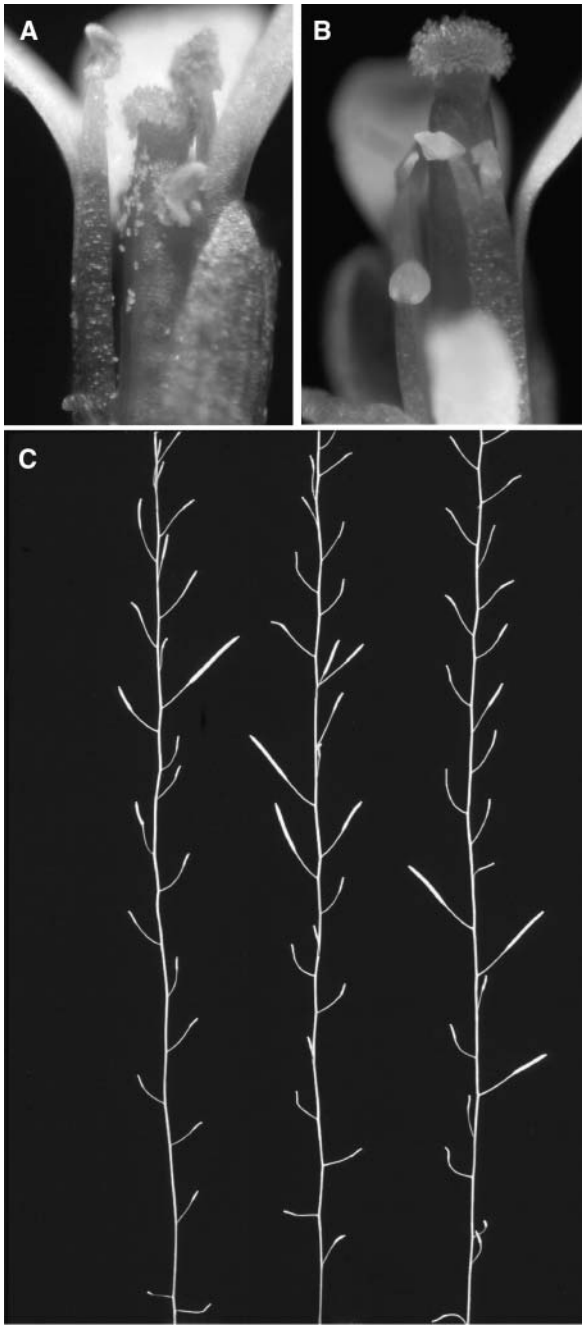

Figure 2. Characteristics of the Male Sterile Phenotype of *myb33 myb65*.

(A) Flowers of the Columbia-0 ecotype photographed under bright-field microscopy.

(B) Flowers of the *myb33 myb65* double mutant, photographed under bright-field microscopy.

(C) Three different bolts of *myb33 myb65* that exhibit the sporadic setting of siliques, where the majority of siliques fail to set any seeds, but occasionally fully or partially filled siliques are set. Bolts are from plants grown at 22°C in a 12-h-day/12-h-night cycle and ~90 μmol·m^{-2}s^{-1} light intensity.

the stage at which anther development is blocked. Sanders et al. (1999) have divided anther development into 14 stages, at which distinctive cellular events can be visualized at the level of the light microscope.

In *myb33 myb65*, no visible defects were found in early anther development up to stage five (Sanders et al., 1999). Here, the division of the archesporial cells to give rise to the pollen mother cells (PMCs), tapetum, middle layer, and endothecium (Figure 3F) appears indistinguishable from the wild type (Figure 3A). However, during stage six when the PMCs begin to separate in a clearly defined locule and the tapetum begins to vacuolate (Figure 3B), the mutant is similar, except that the tapetum begins to enlarge (Figure 3G). Furthermore, whereas the products of meiosis, the tetrads, become clearly visible in the wild-type anthers (Figure 3C), these structures are not visible in *myb33 myb65*, but rather the tapetum has expanded to such an extent that there is no locule, and the PMCs have an irregular shape (Figure 3H). Thus, the block in pollen development appears to be premeiotic, occurring between anther stages 5 and 6 (Sanders et al., 1999) or floral stages 9 and 10 (Smyth et al., 1990). Whereas microspores form in the locule of wild-type anthers (Figure 3D) and eventually form mature pollen (Figure 3E), the tapetum of the *myb33 myb65* mutant continues to expand (Figure 3I) until the contents collapse and degenerate (Figure 3J). The expansion of the tapetum appears to be due to an increase in cell size, not in cell number.

Such an early and comprehensive block in pollen development in the *myb33 myb65* mutant appears inconsistent with the ability of the mutant to sporadically set partially or completely filled siliques. This apparent paradox was explained by the finding that some anthers from the mutant appear to undergo a wild-type developmental program. Strikingly, individual normal locules can be adjacent to locules in which pollen development has aborted through a hypertrophic tapetum. Figure 4A shows an example of this, where development in the two outer locules is at an early microspore stage, with the tapetum degrading and producing as many microspores as a locule from a wild-type plant (Figure 3D). The wild-type development explains the sporadic fertility of *myb33 myb65*. Thus, although there is some variation in anther development, locules appeared to undertake either one of two predominant courses of development; a completely wild-type developmental program or the tapetum undergoes hypertrophy before meiosis, resulting in the abortion of pollen development. In anthers in which both types of locules were present, there was no consistency in which of the locules of the anther developed normally. This alternative development of locules in the mutant anthers suggests that there are additional factors (environmental or genetic) that are influencing the development of the tapetum and that these factors can have a very localized affect.

To further characterize the mutant, analine blue staining was performed to detect the presence of callose. It was found that *myb33 myb65* could in fact make callose, and similar to the wild type, it accumulates around the PMC at the expected developmental stage (Figure 4B). However, the callose persisted in locules where pollen development had aborted. In Figure 4C, callose is present in the locule that has a hypertrophic tapetum, whereas an adjacent locule that is undergoing a wild-type developmental program has no callose present. The fact that

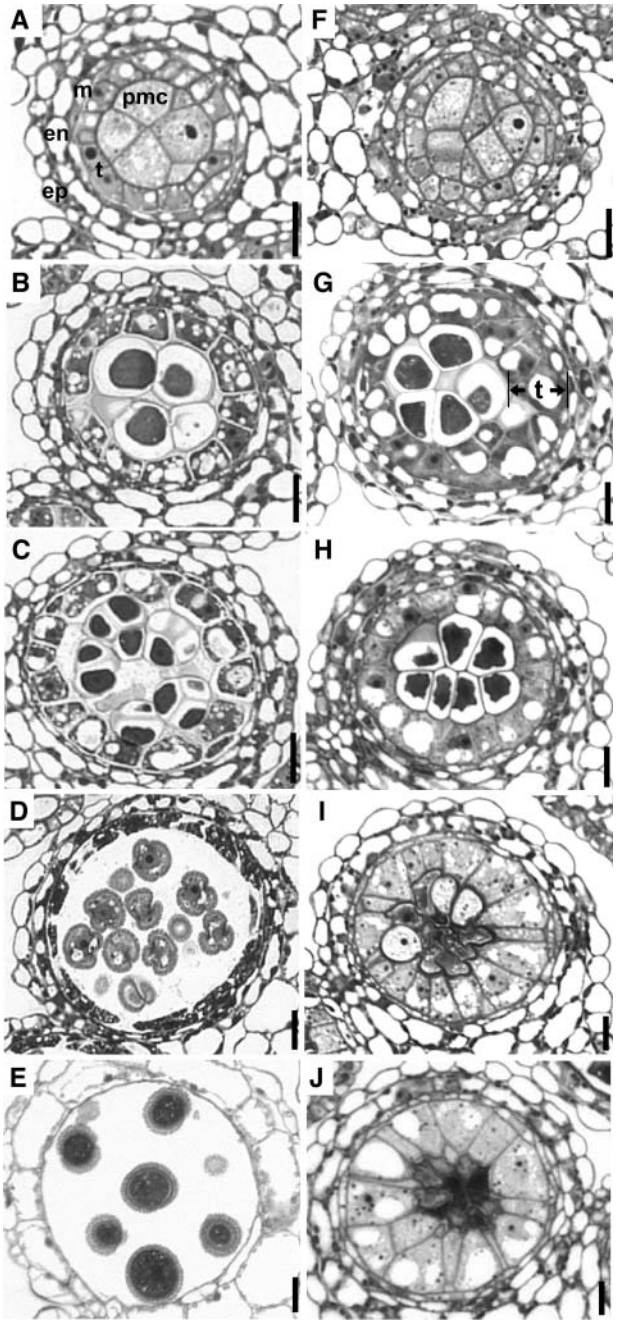

Figure 3. Comparison of the Development of Locules from Wild-Type and *myb33 myb65* Plants Using Toluidine Blue Staining.

(A) to **(E)** Development in wild-type anthers.

(A) Early microsporocyte stage, with the pollen mother cells (pmc) surrounded by the four distinct cell layers, the epidermis (ep), endothecium (en), middle layer (m), and tapetum (t).

(B) PMCs begin to separate from one another and the locular space beginning to form.

(C) Tetrad stage, with the individual microspores separated by callose.

(D) Microspore stage. The tapetum shows signs of degradation and has a granular appearance.

(E) Mature pollen stage (tricellular pollen) before release from the anther. The tapetum has degenerated.

(F) to **(J)** Development in *myb33 myb65* anthers.

(F) Development at the early microsporocyte stage appears indistinguishable from the wild type.

(G) At PMC stage, the tapetum (t) begins to enlarge.

(H) The locule becomes crowded, and the PMCs have an irregular shape.

(I) The tapetum continues to expand, and the PMCs begin to degrade.

(J) The tapetum occupies the majority of the locule, and the PMCs have degenerated.

Anthers are from plants grown at 22°C in a 12-h-day/12-h-night cycle and ~90 $\mu mol \cdot m^{-2}s^{-1}$ light intensity. All bars = 10 μm.

callose is persisting in the defective locule implies that callase has not been secreted from the tapetum and that the tapetum, in addition to undergoing hypertrophy, has ceased performing its normal functions. However, the fact that the other locule has been able to degrade its callose (Figure 4C) implies that the persistence of callose in the aborted locule is a secondary effect, rather than the primary cause of the locule aborting pollen production. The production of callose and its persistence are consistent with the block in development occurring before meiosis, for in the wild type, only after the tetrads are formed is the callose degraded.

Fertility Is Restored in *myb33 myb65* Plants Grown under Higher Light Intensities or at a Lower Growth Temperature

The fact that the double mutant could sporadically set seed and the extent to which it could was highly variable suggested that environmental factors could be influencing the plant's fertility. Light intensity, daylength, and growth temperature can all influence the fertility of a plant (Kaul, 1988). To assess the affect of light intensity on fertility, *myb33 myb65* plants were grown alongside wild-type controls at a light intensity of 95 $\mu mol \cdot m^{-2}s^{-1}$, in a 12-h-day/12-h-night cycle at 22°C. When the plants began to bolt, plants were moved to either 140, 210, or 330 $\mu mol \cdot m^{-2}s^{-1}$ photo intensities as well as being kept at 95 $\mu mol \cdot m^{-2}s^{-1}$. Plants were then allowed to grow for 5 weeks, and fertility was scored by determining the total number of siliques that set seed of each plant, divided by the total number of siliques of the plant, including the empty siliques.

The increased light intensity had a dramatic effect on the number of siliques that wild-type plants produce; at 330 $\mu mol \cdot m^{-2}s^{-1}$, plants produce more than twice as many siliques than at 95 $\mu mol \cdot m^{-2}s^{-1}$ (Table 1). However, if fertility is defined as the percentage of siliques that set seed, there was no significance different in wild-type plants grown under the four different light intensities. By contrast, the double mutant plants produced more than four times as many siliques as Wassilewskija (Ws) at 95 $\mu mol \cdot m^{-2}s^{-1}$, for similar to other male sterile mutants, they go into a phase of continuous flowering because of the inability to set seed. However, the total number of siliques that set seeds, along with the percentage of siliques that set seed, dramatically increased with increased light intensity. Less than four percent of *myb33 myb65* siliques set seed

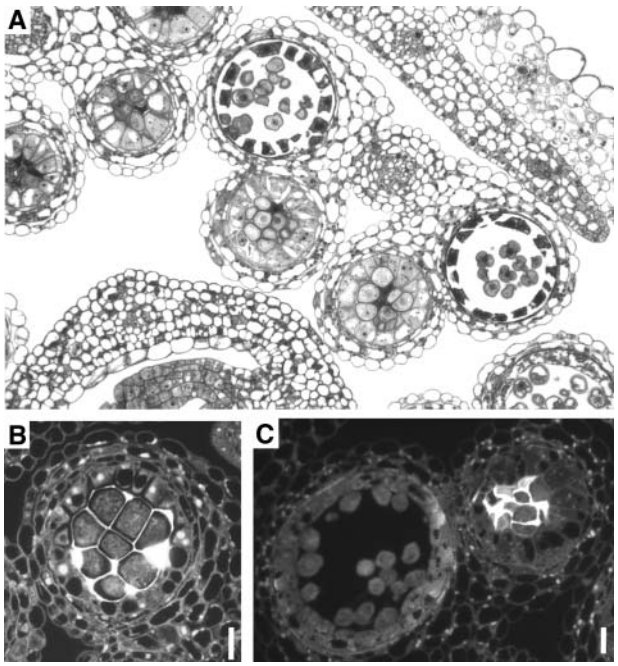

Figure 4. Further Microscopic Analysis of *myb33 myb65* Anthers.

(A) Toluidine blue staining of a section showing the alternative developmental pathways within locules from the same *myb33 myb65* anther.
(B) Alaline blue staining for callose in *myb33 myb65* at the PMC stage under dark-field microscopy. Fluorescence indicates the presence of callose.
(C) Staining for callose in *myb33 myb65* at the microspore stage. Wild-type development has proceeded in the locule on the left (no callose), whereas development has aborted in the locule on the right (callose present).
Anthers are from plants grown at 22°C in a 12-h-day/12-h-night cycle and ~90 μmol·m^{-2}s^{-1} light intensity. All bars = 10 μm.

at 95 μmol·m^{-2}s^{-1}, in comparison with 75% at 330 μmol·m^{-2}s^{-1} (Table 1). Thus, *myb33 myb65* plants are almost as fertile as wild-type plants when grown at a light intensity of 330 μmol·m^{-2}s^{-1}.

The fertility of *myb33 myb65* is also influenced by temperature. Again, plants were grown at 22°C until they began to bolt. Plants were then either left at 22°C or shifted to 16°C at approximately the same light intensity of 86 μmol·m^{-2}s^{-1} (86.9 μmol·m^{-2}s^{-1} at 22°C and 85.5 μmol·m^{-2}s^{-1} at 16°C). Fertility was scored after 5 weeks for the plants grown at 22°C and at 7 weeks for the plants grown at 16°C because of the slower growing conditions. At 22°C after 5 weeks, the *myb33 myb65* plants had produced more than four times as many siliques as Columbia (Col) or Ws, but only 2.5% of these siliques set seed. At 16°C after 7 weeks, the *myb33 myb65* plants were producing similar amounts of siliques as the wild-type controls, Col and Ws, and this reflected the fact that fertility had increased in the *myb33 myb65* plants, for >30% of their siliques had set seed (Table 2). Thus, fertility was >10-fold higher at 16°C relative to 22°C, implying that temperature has a dramatic effect on fertility of the *myb33 myb65* plants.

MYB33 and *MYB65* Promoter-*GUS* Fusions Direct Identical Expression Patterns, but Not in Anthers

Previously, Gocal et al. (2001) examined the expression patterns of *MYB33* and *MYB65* using RNase protection assays and RNA in situ analyses. To extend these studies, promoter-*GUS* fusions, *Pro$_{33}$*:*GUS* and *Pro$_{65}$*:*GUS* (Figure 5B; see Methods), were transformed into Arabidopsis, multiple transgenic plants were obtained, and >12 independent lines were examined for each construct at various stages of development.

GUS staining in *Pro$_{33}$*:*GUS* plants was strongest in the inflorescence and root tips (Figures 6A to 6D). At approximately floral stage 12 (petals level with long stamens; Smyth et al., 1990), the upper half of the pistil stained strongly, with weaker staining in the sepals and the anther filament (Figure 6A). However, no obvious GUS staining was observed in the anther tissues (Figures 6A and 6G). As the flower develops (Figures 6B and 6C), not only does the GUS staining persist in the sepals and upper half of the pistil, but it becomes much stronger in the anther filament and connective. Furthermore, there was strong staining in the receptacle (abscission zone). Thus, the *MYB33* promoter directs GUS expression in the inflorescence in a very complex pattern, and no variation was seen amongst the transgenic lines. Although no GUS staining could be found in mature leaves or stems of plants, GUS staining could be seen in newly emerging leaves, predominantly at the proximal side (Figure 6F). Furthermore, wounding could induce GUS expression, either by crushing cells with a pair of forceps or slicing with a razor blade (Figure 6E, arrow). The response was very local, where GUS was expressed as a narrow band that encircled the wounded site, several cell layers away from the actual wound (Figure 6E). Furthermore, this induction of GUS occurs immediately after wounding, implying that the gene is rapidly induced.

For the *Pro$_{65}$*:*GUS* construct, 2145 bp upstream of the *MYB65* ATG start codon was used. Sequence comparisons between this 2145-bp region to the 2051-bp *MYB33* 5′ region revealed that the first 73 bp immediately 5′ of the ATG of *MYB33* shares significant homology to the corresponding region of the *MYB65* gene. However, beyond this region, the sequences share little homology with one another, with only eight stretches of sequence with six or more base pairs that are identical. However, despite these highly divergent promoter regions, the pattern of GUS expression in *Pro$_{65}$*:*GUS* transgenic plants was identical to that of the complex expression pattern of *Pro$_{33}$*:*GUS* (data not shown) and was again not expressed in anthers.

The 3′ Region of *MYB33* Does Not Direct Expression in Anthers

For correct expression, several genes have been shown to require their 3′ flanking sequences, for regulatory elements can reside in these regions (e.g., Larkin et al., 1993; Chen et al., 1998). Thus, we subcloned the 3′ noncoding sequences of *MYB33*, downstream of the *GUS* gene into the *Pro$_{33}$*:*GUS* construct, resulting in the construct *Pro$_{33}$*:*GUS*:*3′end* (Figure 5C). This fragment contains all sequences 3′ of the coding region of *MYB33* to the next open reading frame downstream. Transgenic plants displayed a GUS expression pattern that was identical, both

Table 1. Fertility in *myb33 myb65* Increases with Light Intensity

Ecotype/Mutant	Light Intensity (μmol·m^{-2}s^{-1})[a]	Total Number of Siliques/Plant	Total Number of Filled Siliques/Plant	Percentage of Filled Siliques
Ws				
	95	55.0 ± 4.7	52.6 ± 4.7	96.2 ± 1.1
	140	51.7 ± 12.2	49.4 ± 11.7	96.2 ± 1.3
	210	99.3 ± 11.1	95.5 ± 10.5	96.2 ± 0.6
	330	152.7 ± 15.3	152.6 ± 15.3	97.6 ± 0.5
Col				
	95	39.8 ± 6.7	35.0 ± 5.3	89.3 ± 1.5
	140	61.8 ± 10.0	57.8 ± 9.4	93.3 ± 1.9
	210	103.7 ± 11.2	97.5 ± 11.0	93.3 ± 1.7
	330	83.0 ± 10.9	75.1 ± 10.9	89.9 ± 3.4
myb33 myb65				
	95	241.6 ± 37.7	7.1 ± 1.2	3.6 ± 0.9
	140	129.6 ± 16.8	46.3 ± 7.13	35.5 ± 3.7
	210	203.0 ± 39.2	107.3 ± 29.2	50.3 ± 3.5
	330	176.1 ± 23.0	136.0 ± 21.1	75.1 ± 2.6

[a] Light intensity at which the plants were grown.

spatially and temporally, to *Pro$_{33}$*:*GUS* and *Pro$_{65}$*:*GUS*, and again no expression was seen in anthers, suggesting that sequences 3′ of the *MYB33* coding region do not contain regulatory elements that control tissue-specific expression.

The *myb65* Allele Contains an Enhancer Trap That Expresses GUS Similar to the Promoter-*GUS* Lines

The *myb65* allele was generated using the binary vector pD991 that contains a minimal promoter fused to the *GUS* reporter gene (Figure 1B), and this can act as an enhancer trap (Campisi et al., 1999). The *myb65* plants only had one T-DNA locus; thus, any *GUS* gene expression will be driven by regulatory elements of the *MYB65* gene. When *myb65* mutant plants were stained for GUS activity, a similar pattern of spatial and temporal expression was observed as the *Pro$_{33}$*:*GUS* and *Pro$_{65}$*:*GUS* lines. Staining was strongest in mature flowers, with sepals, receptacle, anther filaments, and connective all staining for GUS activity (Figure 6H). The fact that both the enhancer trap line and the *Pro$_{33}$*:*GUS* and *Pro$_{65}$*:*GUS* lines stain identically in these tissues would argue that *MYB33*/*MYB65* are genuinely expressed in these locations. However, there were several differences between the enhancer trap and promoter-*GUS* lines. First, in female tissues, GUS staining was absent from the stigma/style, but some staining did appear in the ovules (Figure 6H). Furthermore, expression in the enhancer trap line was not wound inducible.

In Floral Tissues, a *MYB33*:*GUS* Translational Fusion Is Expressed Exclusively in Young Anthers

Neither the *Pro$_{33}$*:*GUS*/*Pro$_{65}$*:*GUS* lines or the enhancer trap line had any GUS staining in anthers, despite the phenotype of *myb33 myb65* and the RNA in situ data suggesting *MYB33*/*MYB65* was expressed in young anthers (Gocal et al., 2001). Thus, we constructed a *MYB33*:*GUS* translational fusion (Figure 5E) using the whole *MYB33* gene (pPZP-*MYB33*, Figure 5A) that could fully complement the *myb33 myb65* mutant, implying all the regulatory sequences required for anther development are present.

In stark contrast with the promoter-*GUS* lines and enhancer trap line, expression in flowers was found to only be located in young anthers (Figure 6I) in >24 independent lines examined. No expression could be seen in the rest of the flower, including

Table 2. Lower Growth Temperature Partially Restores Fertility in *myb33 myb65*

Growth Temperature[a]	Ecotype/Mutant	Total Number of Siliques/Plant	Total Number of Filled Siliques/Plant	Percentage of Filled Siliques
22°C	Col	51.6 ± 5.5	45.9 ± 3.9	91.2 ± 2.0
	Ws	49.7 ± 5.0	45.8 ± 4.3	92.8 ± 1.4
	myb33 myb65	217.1 ± 14.8	5.0 ± 1.9	2.5 ± 0.7
16°C	Col	101.3 ± 29.0	87.8 ± 24.2	89.6 ± 2.5
	Ws	154.4 ± 13.1	152.4 ± 13.2	98.4 ± 0.8
	myb33 myb65	112.3 ± 10.0	36.4 ± 5.4	32.5 ± 3.4

[a] Temperature at which the plants were grown.

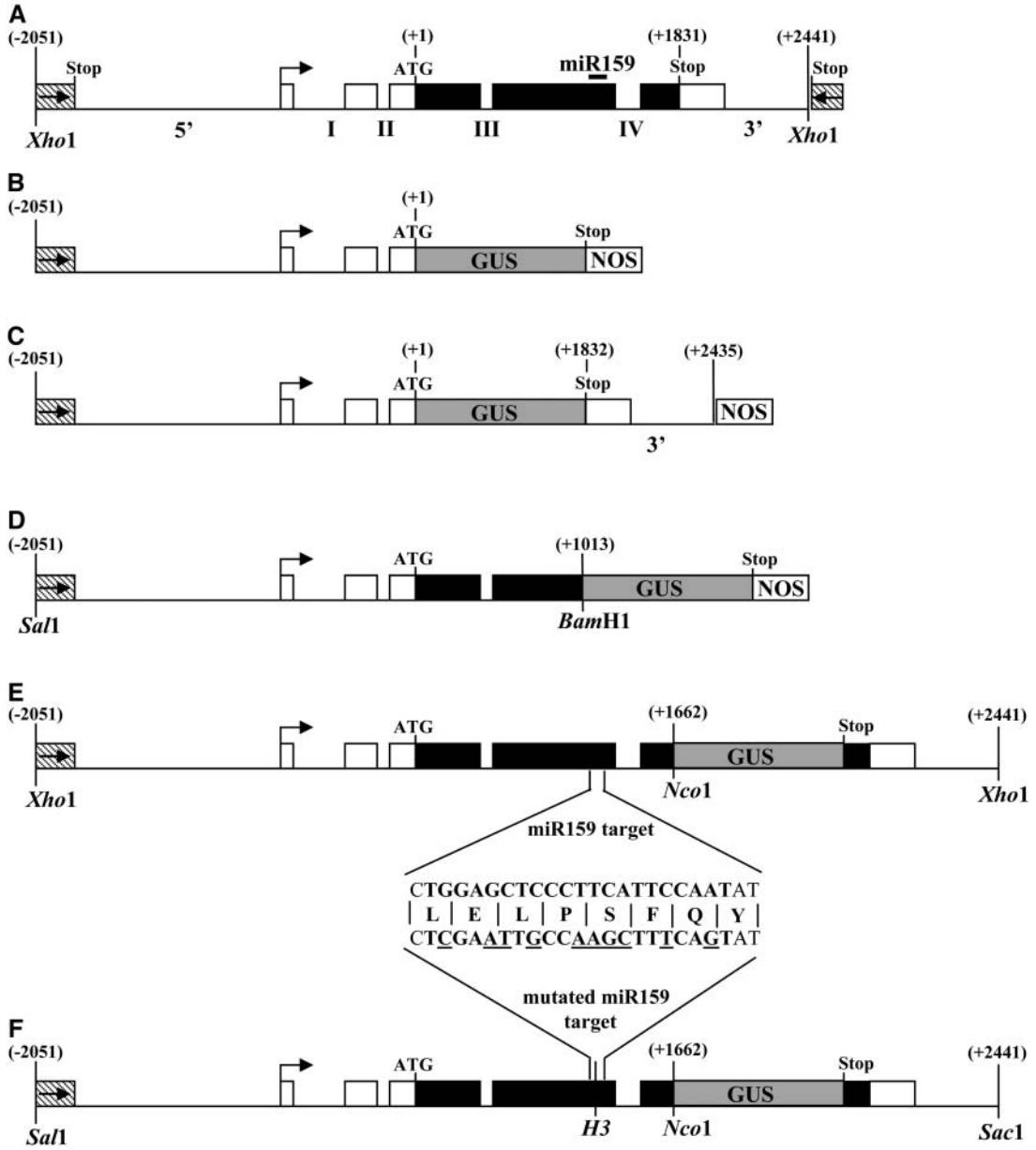

Figure 5. Structure of the Constructs Used for Molecular Complementation, for *MYB33* Expression Analysis, and for Overexpresion of *MYB33* and *mMYB33* Genes.

(A) Structure of the Landsberg *erecta MYB33* genomic clone used for molecular complementation. This clone contains 1390 bp upstream of the putative transcription start site (arrow), which includes all the 5′ untranscribed regions of *MYB33* and into the coding region of the upstream gene (At5g06090; the stop codon being −1833 relative to *MYB33* start codon), 660 bp of 5′ untranslated region, including the first two introns (denoted I and II), 1833 bp of open reading frame, including two introns (denoted III and IV), and 611 bp of sequences 3′ of the *MYB33* stop codon, which extends downstream 12 bp before the stop codon of the next gene (At5g060110; stop codon is +624 bp relative to *MYB33* stop codon). Untranscribed regions and introns are shown as thin lines, untranslated regions as open boxes, and coding regions as closed boxes. Numbers shown are relative to the *MYB33* start codon. The location of the miR159 target is indicated by a solid line. This construct was also used to overexpress *MYB33* in wild-type plants.

(B) The Pro_{33}:*GUS* transgene in the vector pBI101.1.

(C) The Pro_{33}:*GUS*:*3′end* transgene in the vector backbone pBI101.1

(D) The *5′-MYB33*:*GUS* transgene in the vector backbone pBI101.1.

(E) The *MYB33*:*GUS* transgene made in the vector pPZP200-Hygro.

(F) The *mMYB33*:*GUS* transgene made in the vector pPZP200-Hygro. The alteration to the nucleotide sequence in the miRNA target motif is shown, and nucleotides underlined are those differing from the wild type. The unaltered amino acid sequence is shown. The *mMYB33* gene is identical but lacks the *GUS* reporter gene. H3, *Hin*dIII.

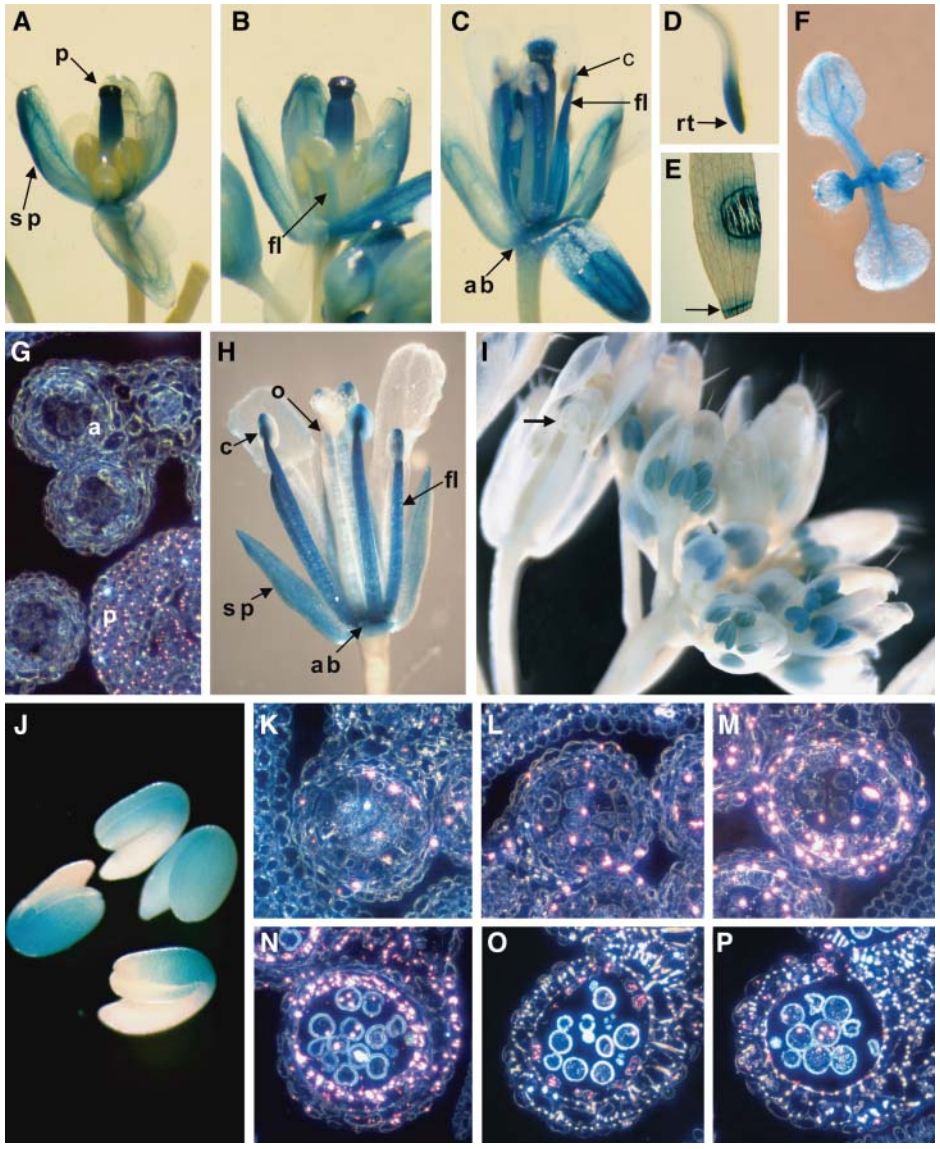

Figure 6. Expression of *MYB33* and *MYB65*; GUS Staining of Transgenic *Pro*$_{33}$:*GUS*, *myb65* Enhancer Trap, and *MYB33*:*GUS* Arabidopsis Plants.

(A) GUS activity as determined by histochemical analysis in a *Pro*$_{33}$:*GUS* Arabidopsis flower at floral stage 12.
(B) *Pro*$_{33}$:*GUS* flower at floral stage 13.
(C) *Pro*$_{33}$:*GUS* flower at floral stage 15.
(D) *Pro*$_{33}$:*GUS* root of a 5-d-old plant.
(E) Wounded leaf of a *Pro*$_{33}$:*GUS* plant.
(F) Seven-day-old *Pro*$_{33}$:*GUS* seedling
(G) Transverse section of young anthers at the PMC stage of *Pro*$_{33}$:*GUS* shown under dark-field microscopy. Pink crystals indicate GUS expression.
(H) A GUS-stained flower (at floral stage 15) from the *myb65* enhancer trap line.
(I) A GUS-stained inflorescence of a *MYB33*:*GUS* plant.
(J) GUS-stained imbibed seeds from a *MYB33*:*GUS* plant.
(K) Transverse section of *MYB33*:*GUS* anthers at the archesporial cell stage.
(L) Early PMC stage.
(M) Meiosis.
(N) Young microspore stage.
(O) Stage of tapetal degeneration.
(P) Dehiscence.
a, anther; ab, abscission zone (receptacle); c, connective; fl, anther filament; o, ovule; p, pistil; rt, root tip; sp, sepal.

sepals, receptacle, anther filaments, and stigma/style at any stage, and expression was not wound inducible. Expression was strongest in anthers before floral stage 12 (Smyth et al., 1990); however, after this developmental stage, expression appeared to be absent (arrow, Figure 6I). Expression from the transgene was generally low, and most lines required >30 h of incubation for strong staining. Expression was also found in imbibed seeds, being strongest in the region where the cotyledons met the hypocotyl (Figure 6J).

To analyze the spatial and temporal pattern of *MYB33*:*GUS* expression in anthers, inflorescences were fixed and sectioned transversely. Expression of GUS is shown as pink crystals, with the level of expression reflected in the number and size of the crystals. Through all stages of development, GUS crystals were only observed in anthers. GUS crystals were visible at the archesporial cell stage; however, their number was low and was mainly confined to the four anther cell layers (Figure 6K). Expression increased slightly at the PMC stage (Figure 6L), and at meiosis when the tetrads became visible, expression increased dramatically in the four anther cell layers (Figure 6M) and was also found in the connective region (data not shown) and the tetrads themselves. After this developmental stage, GUS expression remained strong but is mainly confined to the tapetum (Figure 6N), and expression persists in this cell layer until it degrades (Figure 6O). At dehiscence, low levels of expression are found in the pollen grains and in the epidermis, adjacent to the stomium (Figure 6P).

Posttranscriptional Regulation of *MYB33*/*MYB65*: An miR159 Target Sequence Restricts Expression to Anthers

The promoter-*GUS* constructs and the *MYB33*:*GUS* translational fusion generate dramatically contrasting expression patterns. A possible explanation for this is that sequences are present downstream of the ATG (+1) that repress expression in tissues outside the anther (i.e., sepals, anther filaments, receptacle, stigma/style, roots, and wounding). One potential sequence is the miR159 target motif that is fully conserved between *MYB33* and *MYB65* (Figure 7A). Furthermore, this motif is highly conserved amongst the other closely related Arabidopsis *MYB* genes and in all cereal *GAMYB* genes cloned to date (Figure 7A). This high level of conservation implies that this motif plays an important role in the function of these *MYB* genes.

To test the importance of the miR159 target sequence for *MYB33* expression, or whether other regulatory sequences are present downstream of the ATG (+1), two different constructs were made. First, a construct was made, *5′-MYB33*:*GUS*, where the *MYB33* promoter, along with the first 1013 bp of the *MYB33* gene, was fused in frame with the *GUS* reporter gene (Figure 5D). This includes all the sequences to 10 bp 5′ of the miR159 target motif. Multiple *5′-MYB33*:*GUS* transgenic plants were generated, and >16 independent primary transformants were analyzed. All lines had a pattern of GUS expression that was indistinguishable from that of Pro_{33}:*GUS*, Pro_{65}:*GUS*, and Pro_{33}:*GUS*:*3′end*. Furthermore, the strength of GUS activity is also similar; thus, it appears that there are no regulatory motifs, downstream of the ATG and upstream of the miR159 target sequence, that are regulating expression of the gene.

The second construct, *mMYB33*:*GUS*, is identical to *MYB33*:*GUS*, except that the miR159 target site has been mutated, altering the sequence of 10 nucleotides, but not the amino acid sequence the region encodes (Figure 5F; Palatnik et al., 2003). Multiple transgenic plants harboring this *mMYB33*:*GUS* construct were generated, and inflorescences from 16 different primary transformants were stained for GUS expression. There was variation in the pattern of GUS expression in the different primary transformants. For seven lines, weak GUS expression was found to be specifically in young anthers identical to *MYB33*:*GUS*. For seven other lines, much stronger expression was found, and in addition to expression being in young anthers, the expression pattern had increased in tissues outside the anther (Figure 7C), similar to the spatial and temporal expression of the promoter-GUS lines (Figures 6A to 6F). This included the upper half of the pistal throughout flower development, the receptacle, anther filaments, and connective, but a lack of expression in anther themselves after floral stage 12, with some expression in stems (Figure 7C). Furthermore, wounding induced GUS expression. Thus, the expression pattern of *mMYB33*:*GUS* resembled a combination of Pro_{33}:*GUS* and *MYB33*:*GUS*, demonstrating that these two expression patterns were not mutually exclusive.

Expression was also examined in seedlings. Seeds from 16 different *mMYB33*:*GUS* lines were planted alongside eight *MYB33*:*GUS* lines and eight *5′-MYB33*:*GUS* lines and were stained for GUS activity after 3 and 7 d of germination. After 3 d of germination, all *mMYB33*:*GUS* lines had strong GUS expression in root tips in all but two lines, and expression was also seen in the cotyledons of the strongest expressing lines (Figure 7B). GUS expression was seen in all eight *5′-MYB33*:*GUS* lines examined, and typically stained stronger than *mMYB33*:*GUS* lines. By contrast, there was no GUS staining in any of the eight *MYB33*:*GUS* lines. In 7-d-old *mMYB33*:*GUS* seedlings, expression was still found in root tips, in both primary and secondary roots. Furthermore, expression was seen in and around the shoot meristem and in the proximal regions of the young emerging true leaves (Figure 7E). A similar pattern of expression was seen in the *5′-MYB33*:*GUS* lines (Figure 7F). In contrast with the *mMYB33*:*GUS* and *5′-MYB33*:*GUS* lines, no GUS was seen in any of eight *MYB33*:*GUS* lines examined (Figure 7D), even after 48 h of staining.

Thus, in conclusion, mutation of the miR159 target sequence results in increased expression of *MYB33* in tissues outside the anther, and these are tissues in which the promoter-*GUS* lines were seen to be directing expression (Figure 6). This suggests that the miR159 target sequence restricts the expression pattern of *MYB33*.

Introduction of *mMYB33* into Plants Results in Dramatic Pleiotrophic Developmental Defects

The altered expression pattern of *mMYB33*:*GUS* suggests that the miR159 target sequence is important for restricting the domain of *MYB33* expression. To investigate whether expression of *MYB33* in these tissues outside the anther have consequences for plant growth and development, we transformed Arabidopsis with the *mMYB33* construct, which is identical to

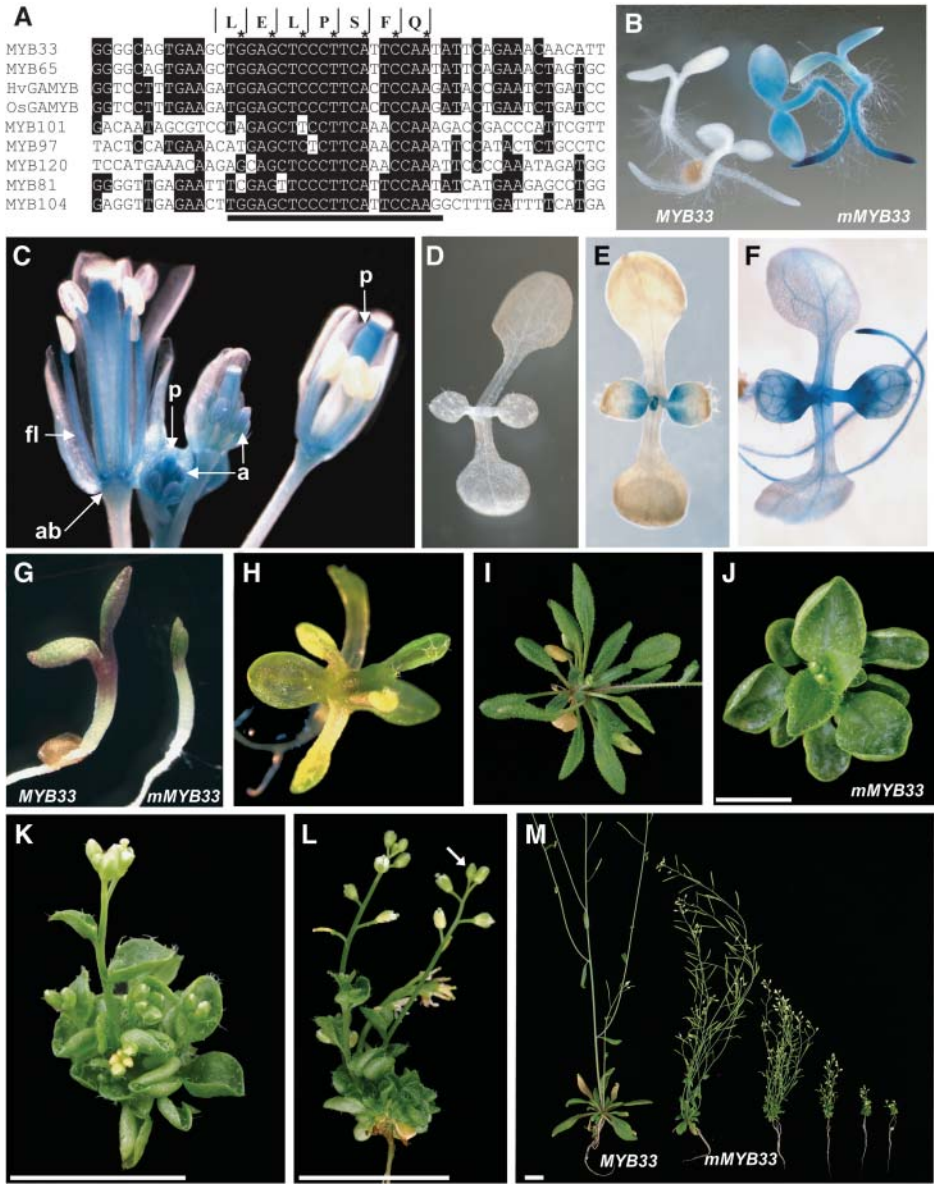

Figure 7. The miR159 Target Motif Is Highly Conserved and Is Required to Restrict *MYB33* Expression for Normal Plant Development.

(A) Alignment of the miR159 target sequence (black line) and surrounding sequences of the *GAMYB-like* genes of Arabidopsis (*AtMYB33*, *AtMYB65*, *AtMYB101*, *AtMYB97*, and *AtMYB120*), as well as two other closely related genes (*AtMYB81* and *AtMYB104*), and the barley (*HvGAMYB*) and rice (*OsGAMYB*) genes. Amino acid sequence above corresponds to the sequence encoded by *MYB33* and *MYB65*. The asterisk indicates the third position in each codon.

(B) GUS staining of 3-d-old *MYB33*:*GUS* and *mMYB33*:*GUS* seedlings.

(C) GUS staining of an inflorescence from a *mMYB33*:*GUS* transgenic line.

(D) GUS staining of a 7-d-old *MYB33*:*GUS* seedling (48 h of staining).

(E) GUS staining of a 7-d-old *mMYB33*:*GUS* seedling (16 h of staining).

(F) GUS staining of a 7-d-old *5′-MYB33*:*GUS* seedling (6 h of staining).

(G) Comparison of 5-d-old transgenic plants transformed with the wild-type *MYB33* gene (left) and *mMYB33* (right).

(H) Ten-day-old *mMYB33* transformant that is failing to form proper leaves.

(I) Rosette of a 4-week-old plant transformed with the *MYB33* gene.

(J) Rosette of a 4-week-old plant transformed with the *mMYB33* gene.

(K) Side view of a 3-week-old *mMYB33* plant exhibiting extreme leaf curling.

(L) Side view of a 4-week-old *mMYB33* plant exhibiting a short primary bolt with a terminal flower.

(M) Comparison of a 4-week-old *MYB33* transformant with *mMYB33* transformants with phenotypic defects of increasing degrees.

ab, abscission zone; a, anther; fl, anther filament; p, pistal. Bars = 1 cm.

mMYB33:*GUS*, but lacking the *GUS* reporter gene (see Methods). For comparison, Arabidopsis transformants were also generated with the wild-type *MYB33* gene (the pPZP-*MYB33* construct).

For the *MYB33* gene, 82 primary transformants were obtained and transferred to soil. Of these, two plants had a spindly/dwarf stature, and four others appeared male sterile. The phenotype of the other 76 appeared completely wild-type. For the *mMYB33* construct, 74 primary transformants were obtained and transferred to soil. Many of these 5-d-old seedlings appeared to have developmental defects, with the cotyledons failing to expand (Figure 7G), and in 10-d-old seedlings, many plants had first true leaves that had unusual morphology (Figure 7H). Of the 74 plants, 62 survived, with only four plants having a phenotype resembling wild-type plants. The 12 plants that died indicated that expression of this gene results in seedling arrest. The remainder had mutant phenotypes with common developmental characteristics, but to differing degrees (Figure 7M). All the 58 mutant plants had a reduced size, with 11 plants having a rosette of <1 cm in diameter, and 44 plants having a diameter of <2 cm. The smaller the rosette, the shorter the bolts (shorter internode lengths) and the more reduced the apical dominance, indicating there was a general negative effect on plant growth. This was also the case with fertility, with the most severe transformants failing to set seed, whereas the less severe transformants had fully extended siliques. In all *mMYB33* plants, leaves were profoundly more rounded than the wild type (cf. Figure 7I with 7J) and upturned at the sides (Figures 7J to 7L), petiole lengths were dramatically reduced (Figure 7J), and many had short bolts with terminal flowers (Figure 7L, arrow). Again these phenotypic characteristics were more pronounced in plants with the most stunted phenotype. All these characteristics were different in the two spindly/dwarf plants obtained with the *MYB33* gene. Thus, it appears expression of *MYB33*, in which the miR159 target sequence has been mutated, has dramatic consequences for plant growth and development.

DISCUSSION

MYB33 and *MYB65* Redundantly Facilitate Anther Development

Using a reverse genetic approach, we have shown a role for *MYB33* and *MYB65* in anther development. The fact that neither single mutant displayed a phenotype, whereas the *myb33 myb65* double mutant was male sterile, implies that *MYB33* and *MYB65* are functionally redundant, which was not surprising considering the high homology they share and the fact that these genes lie within segmental chromosomal duplications. *MYB33* and *MYB65* have been previously coined the *GAMYB-like* genes, for they have high homology to *HvGAMYB* and evidence suggested that they were mediating the GA signal in plants (Gocal et al., 2001). A role in anther development is consistent with transducing a GA signal, for GA is known to control anther development (Jacobsen and Olszewski, 1991; Goto and Pharis, 1999) and HvGAMYB expression in barley anther increases after GA_3 application (Murray et al., 2003).

The premeiotic block in *myb33 myb65* anther development results from tapetal hypertrophy. The tapetum is a critical tissue, mediating between the gametophyte and sporophyte, and this is highlighted across the plant kingdom in that tapetal malfunction is regarded as the prime cause of male sterility, from either environmental or genetic causes (Kaul, 1988). In Arabidopsis, four male sterile mutants in which the tapetum undergoes hypertrophy have been described; *ms3* (Chaudhury et al., 1994), *fat tapetum* (Sanders et al., 1999), *gne1* and *gne4* (Sorensen et al., 2002). In each case, hypertrophy occurs at the onset of meiosis similar to *myb33 myb65*. However, unlike *myb33 myb65*, in all these mutants, middle layer hypertrophy also occurs, and this along with the enlarged tapetum appears to crush the microsporocytes, resulting in their degeneration. Thus, *myb33 myb65* is different with respect that only one microsporangial cell layer is affected, the tapetum, with the size of the middle layer remaining the same as the wild type. Also, in these previous Arabidopsis mutants, the tapetum degenerates leaving an empty locule that eventually results in a collapsed anther wall. In *myb33 myb65* plants, the tapetum shows no sign of degeneration.

Consistent with the phenotype of *myb33 myb65*, the expression of a *MYB33*:*GUS* transgene was confined in the floral tissues to anthers, predominantly in the tapetum at meiosis, the developmental stage at which hypertrophy begins. However, this expression is not essential for anther development, for in *myb33 myb65*, adjacent locules of the same anther can undergo different developmental programs; either the tapetum undergoes hypertrophy just before meiosis or the anther develops normally. This stage-specific developmental decision is greatly influenced by environmental factors, where under conditions of favorable growth (16°C [low temperature] or 300 $\mu mol \cdot m^{-2}s^{-1}$ [high light]), fertility of *myb33 myb65* can be restored to almost wild-type levels. When we consider our standard growth conditions of 90 to 100 μmol light intensity, this would be regarded as low light intensity, whereas 22°C for a temperate plant as Arabidopsis could be considered as moderately high. Thus, the conditions that restore fertility in *myb33 myb65* would probably be closer to the conditions Arabidopsis encounters in its natural environment. In this respect, the expression of *MYB33*/*MYB65* could be considered as limiting in the anther under poor environmental conditions. Curiously, both the conditions that restore fertility, high light and lower growth temperature, result in higher levels of soluble carbohydrates in the plant (Hurry et al., 1995), and the *MYB33* gene is being expressed in the tapetum at the time when tapetal carbohydrate (starch) reserves are being mobilized, just before meiosis (Clement et al., 1994). Although it is tempting to speculate that these *MYB* genes may play a role similar to HvGAMYB in barley aleurone (starch mobilization), further investigation is needed to elucidate the conditional nature of *MYB33*/*MYB65* in the anther and alternative possibilities, such as further redundancy with other *GAMYB-like* homologs.

Rice *gamyb* mutants are blocked at a similar stage in anther development as *myb33 myb65*, where just before meiosis, the tapetum undergoes hypertrophy (Kaneko et al., 2004). Furthermore, the extent of sterility is variable, where it has been noted that greater sterility occurs at higher temperatures (Kaneko et al., 2004). The major difference in *gamyb* plants appears to be that other floral organs are also affected by this mutation. In barley,

overexpression of *HvGAMYB* in transgenic plants also leads to a male sterile phenotype; however, the pollen developed normally, but dehiscence fails to occur, with the septum failing to rupture (Murray et al., 2003). Lastly, similar to Arabidopsis, GAMYB in both rice and barley is expressed in anthers (Murray et al., 2003; Kaneko et al., 2004). So both the expression and function of GAMYB in anther development appears to be highly conserved between Arabidopsis and cereals.

Analysis of the Control of *MYB33* Expression

The dramatically contrasting expression patterns we obtained with our different reporter gene constructs highlights the complexities underlying the regulation of *MYB33*. The presence of the miR159 binding site within the *MYB33* gene can explain why expression in *MYB33*:*GUS* plants is repressed in certain tissues, but it cannot explain the lack of expression in anthers of the promoter:GUS lines. Our experiments have enabled us to propose a model for the tissue-specific control of *MYB33* expression (Figure 8). First, the 5′ upsteam region (*Pro*$_{33}$:*GUS*) directs expression in flowers (receptacle, anther filaments/connective, pistal, and sepals), shoot apices, and root tips. The addition of region A (*5′-MYB33*:*GUS*) or region C (*Pro*$_{33}$:*GUS*:*3′end*) alone does not alter the expression pattern (Figure 8). However, when they are present along with region B (*mMYB33*:*GUS*), they are sufficient for anther expression. Thus, either region B contains specific sequences required for anther expression, or a combination of all regions or subset of regions is required for anther expression. The only sequence we can exclude from being required for anther development is the miR159 binding site, for in *mMYB33*:*GUS* and another construct in which the miR159 binding site had been deleted (A.A. Millar and F. Gubler, unpublished data), expression still occurs in anthers. The fact that expression in the *myb65* enhancer trap lacks expression in anthers and contains all these corresponding regions suggests that these anther-required sequences are not simply *cis*-acting enhancers, but may have to be transcribed or translated to exert

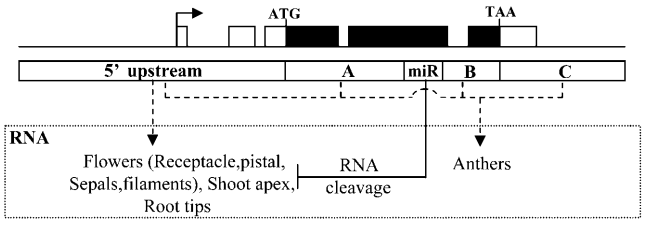

Figure 8. Model for the Control of *MYB33* Expression.

The 5′ upstream region strongly promotes expression in flowers (receptacle, pistal, sepals, and anther filaments/connective), meristems, and root tips. Addition of region A or region C alone does not alter this expression pattern. Addition of these two regions together, along with region B, enables expression in anthers. The miR159 target sequence (miR) represses expression in meristems, root tips, and flowers but has no apparent effect on anthers. Region A, contains sequences from the ATG (+1) to +1024; region B, +1043 to the stop codon (+1832); region C, from the stop codon to the open reading frame of the gene downstream of *MYB33*.

their regulatory effect. Recently, evidence was presented that the *SUPERMAN* gene of Arabidopsis has both positive and negative regulatory elements in its protein-coding region (Ito et al., 2003), and this may be the case for *MYB33*. A second possibility is that some higher-order structure is required, such as a specific chromatin configuration (Lomvardas and Thanos, 2002) and that having any significant disruption, such as a large deletion or insertion of a T-DNA (e.g., the *MYB65* enhancer trap), interferes with the required configuration for anther expression.

MYB33 Is Regulated by miRNAs

By mutating the miRNA target sequence within the *MYB33*:*GUS* gene (*mMYB33*:*GUS*), we have demonstrated visually how the expression pattern of *MYB33* is restricted by miRNAs. They downregulate or silence *MYB33* expression in shoot apices, root tips, and flowers, but not anthers, the only tissue in which we see a phenotype in the *myb33 myb65* mutant. The most likely mechanism of regulation is mRNA cleavage, for miRNA-guided cleavage products have been found both for *MYB33* and *MYB65* (Palatnik et al., 2003), which have been shown to be the result of miR159 expression (Achard et al., 2004). In situ analysis (Gocal et al., 2001) found *MYB33* mRNA in tissues in which *MYB33* is being repressed by miRNAs, such as root tips and shoot apices. Therefore, we would predict that the signal detected in these tissues would predominantly represent cleaved transcript for this technique is unable to distinguish between intact and cleaved mRNA. Thus, in this instance, the *MYB33*:*GUS* transgene may be a more accurate reflection of where MYB33 protein accumulates rather than *MYB33* RNA in situ hybridization.

The strong expression in germinating *mMYB33*:*GUS* seedlings in and around the shoot meristem region and on the proximal periphery of young developing leaves provides a rationale for the phenotype exhibited by *mMYB33* transgenic plants. miR159 must be refining or abolishing the expression of *MYB33* in shoot apices, the tissues from which leaf primordia arise, and gene expression programs are determining leaf size and shape (Kessler and Sinha, 2004). *MYB33* has been hypothesized to be an activator of *LEAFY* (Gocal et al., 2001), and interestingly, *mMYB33* plants do have some characteristics of *35S*::*LEAFY* plants, such as short bolts with terminal flowers (Weigel and Nilsson, 1995). Thus, expression of *MYB33* in the incorrect cells at a crucial time early on in development may be triggering incorrect developmental pathways that culminate in the gross abnormalities observed in the *mMYB33* plants. The seedling arrest in *mMYB33* plants may provide the rationale for the absence of mutants in the *MYB33* miRNA target motif, similar to those leaf developmental mutants recovered for the *PHABULOSA* family (Emery et al., 2003).

The growth retarding effect of the *mMYB33* transgene appears contradictory to the proposed role in mediating a GA signal. Furthermore, the *mMYB33* phenotype appears unrelated to *myb33 myb65* plants or plants overexpressing miR159 under the control of the 35S promoter (Achard et al., 2004). Transgenic *35S*:*miR159a* Arabidopsis was found to have delayed flowering in short-day photoperiods and to be male sterile (Achard et al., 2004). Presumably in wild-type plants, miR159 is not expressed or weaky expressed in anthers, thus allowing *MYB33* expression

in these tissues, and this scenario has been changed in the *35S*:*miR159a* plants. However, *35S*:*miR159a* anthers appeared to be blocked at a different stage of development compared with *myb33 myb65*, for *35S*:*miR159a* anthers increased in size and they darkened in color. This raises the possibility that other members of the Arabidopsis *GAMYB-like* family are targeted by miR159a and they too play roles in anther development.

We designed the mutations in the miR159 target to match those of Palatnik et al. (2003), who also transformed *mMYB33* into Arabidopsis, but under the 35S promoter. Our results confirm some of their findings, such as upwardly curling leaves (Palatnik et al., 2003). However, although a detailed description of the 35S:*mMYB33* plants was not given, there does appear to be significant differences between *mMYB33* and 35S:*mMYB33* plants. For instance, the petiole lengths of *mMYB33* leaves are dramatically reduced when compared with the petioles of 35S:*mMYB33* plants (Palatnik et al., 2003), and such dramatic reductions in plant size were not reported for *mMYB33* plants. Seedling arrest was not reported for the *35S*:*mMYB33* gene, and the frequency of aberration was much higher in *mMYB33* transformants (58 from 62) than in 35S:*mMYB33* transformants (39 from 63; Palatnik et al., 2003). All these data indicate that a much stronger phenotype was produced with the endogenous *MYB33* promoter than the 35S promoter.

One striking observation from comparison of *MYB33*:*GUS* and *mMYB33*:*GUS* plants is the apparent complete abolishment of expression of *MYB33* in certain tissues, most notably in the root tips and the shoot apical meristem. It raises the interesting conundrum of why the gene is expressed in these tissues, but ultimately this expression is silenced or downregulated by miRNAs. Furthermore, from the phenotype of the *mMYB33* plants, if these genes were not regulated correctly, they would be a liability to the plant. The fact that RNA in situ analyses have found *GAMYB* expression not only in meristems of Arabidopsis (Gocal et al., 2001), but also in the meristems of cereals such as Lolium (Gocal et al., 1999) and rice (Kaneko et al., 2004), would argue that *GAMYB* may have a highly conserved function within the meristem. It remains to be seen whether these genes are not silenced by miRNAs in a small group of cells within the meristem. And, as hypothesized by Rhoades et al. (2002), if *MYB33* is a long-lived transcript, one way to abolish its expression in rapidly dividing cells (to allow differentiation) is through miRNA regulation, thus providing a rationale for our observations. However, with the loss-of-function *myb33 myb65* mutant, the only phenotypic alteration we have found is a conditional role in anther development. If *MYB33*/*MYB65* are performing additional roles in Arabidopsis and these roles are masked by further redundancy that may exist within the Arabidopsis *GAMYB-like* gene family, the generation of additional combinations of mutants may be needed to uncover further phenotypes.

METHODS

Isolation of T-DNA Insertional Mutants

Three pools of T-DNA–tagged mutants were screened, the collection at the Arabidopsis Knockout Facility at the University of Wisconsin, which was done as a service, and the Jack and Feldmann collection, which were obtained from the Arabidopsis Biological Resource Center (Columbus, OH). The Madison collection was only screened with the recommended left border primer, JL202. Both the Jack and Feldmann collections were screened with the recommended left and right border primers. The following primers were used to screen the T-DNA–tagged libraries for insertional mutants in the *MYB65* gene, 65-1 (5′-TACCTCAGCTAGGGTTCGTCTTTGTTGTA-3′) and 65-2 (5′-ACCGTTACTTTGCGAGAAGCAAGACCTAA-3′), or the *MYB33* gene, 33-1 (5′-TGTCGTATTTGTCGTTTCTCGATC-3′) and 33-2 (5′-CTAGTCCATGACCATGAGAAGTGAGAACT-3′). After the identification of initial positive, individual plants were isolated through the procedures outlined at the Arabidopsis Knockout Facility at the University of Wisconsin Web site.

Plant Lines and Growth Conditions

The *myb65* mutant described in this article was isolated from the Madison collection (Krysan et al., 1999) and thus was in the ecotype Ws. The *myb33* mutant described in this article was isolated from the Jack collection; thus, it was in the ecotype Col, with a *glaborous1* background mutation. All plants were grown in a mix of 50% compost and 50% gravel. When growing plants for seed, plants were grown in a 21°C temperature growth room under continuous fluorescent illumination that varied from 60 to 100 $\mu mol \cdot m^{-2} s^{-1}$.

Mutant Genotyping

Amplification with the oligonucleotide 33-1 and the T-DNA–specific primer, JL-202, yielded a 2222-bp product in plants containing the *myb33* allele. Amplification using the oligonucleotides 33-1 and 33-2 yielded a 3644-bp product in plants with a wild-type allele of *MYB33* and no product in plants homozygous for the *myb33* allele. Amplification with the oligonucleotide 65-1 and the T-DNA–specific primer, JL-202, yielded a 1084-bp product in plants containing the *myb65* allele. Amplification using the oligonucleotides 65-1 and 65-2 yielded a 2887-bp product in plants with a wild-type allele of *MYB65* and no product in plants homozygous for the *myb65* allele. All PCR reactions were performed in an Eppendorf Mastercycler gradient PCR machine (Hamburg, Germany), using 35 cycles of 94°C for 15 s, 65°C for 30 s, and 72°C for 2 min. PCR reactions were performed using AmpliTaq DNA polymerase (Applied Biosystems, Foster City, CA) according to the specifications of the supplier.

When required, the genotype of lines was verified using DNA gel blot analysis. For the *myb33* allele, a 1893-bp *Eco*RI genomic clone fragment isolated from Col that spanned the T-DNA insertion site in *myb33* would only give one hybridizing band in the wild-type of 1893 bp; however, in the mutant, it would yield two bands, one at ~2.4 kb and the other at 0.8 kb. For genotyping of the *myb65* allele, the probe used was the PCR product derived from the 65-1 and 65-2 primers. For the wild-type gene, it would hybridize to a fragment of 2643 bp, and for the *myb65* mutant allele, two bands would be present, at ~3.0 and 1.0 kb.

Determination of Fertility under Varying Growth Conditions

Seed was germinated on synthetic media and grown for 5 d at 22 °C under continuous light. Twenty seedlings per 10-cm pot were then transplanted into soil and grown under at 22°C in a 12-h-day/12-h-night cycle at a light intensity of ~90 $\mu mol \cdot m^{-2} s^{-1}$. At the onset of bolting, plants were transferred into the various treatments (higher light intensities; 140, 210, or 330 $\mu mol \cdot m^{-2} s^{-1}$) or lower growth temperature. The higher light intensities were performed in the same growth cabinet but were done by moving the plants closer to the lights. Because of the air circulation, there is no temperature gradient within the cabinet. For the lower growth temperature, treatment plants were moved to a different growth cabinet compared with control plants, and light intensities of these two cabinets were almost identical (86.9 $\mu mol \cdot m^{-2} s^{-1}$ at 22°C and 85.5 $\mu mol \cdot m^{-2} s^{-1}$

at 16°C). After a period of growth, fertility was assessed by scoring each silique with respect to whether it set any seeds. Those siliques with no seeds were scored as sterile and those with at least one seed scored as fertile. Fertility was then defined by dividing the number of fertile siliques (per plant) by the total number of siliques (per plant).

The Generation of Binary Vectors and Transgenic Plants

All the following binary vectors were transformed into the *Agrobacterium tumefaciens* strain GV3101 and used to transform *Arabidopsis thaliana* ecotype Col using the floral dip method (Clough and Bent, 1998). For complementation of the *myb33 myb65* mutant, plants were grown under conditions that promoted male fertility (300 μmol·m^{-2}s^{-1}, 16 h day, 16°C). All PCR amplifications for the following vectors were performed using high-fidelity PlatiniumR *Pfx* DNA polymerase (Invitrogen, Carlsbad, CA).

For complementation, a 4492-bp *Xho*I genomic fragment from Landsberg *erecta* containing the entire *MYB33* gene (Figure 5; Gocal et al., 2001) was subcloned into the *Sal*I site of the binary vector pPZP200-hygro (which was pPZP200 [Hajdukiewicz et al., 1994] with a 35S-hygromycin resistance gene inserted into an end-filled *Eco*RI site of the vector), resulting in construct pPZP-*MYB33*. The primers 2G (5′-CTGAAGGCGGGAAACGACAATCTGATCCA-3′) and *MYB33-2* g (5′-GCAGCTTATGAAGACAATCCTTTTGGT-3′) were used to confirm the presence of the pPZP-*MYB33* transgene in transgenic plants.

For the p*Pro$_{33}$*:*GUS* construct, the 2051 bp immediately upstream of the ATG of *MYB33* was PCR amplified from *MYB33* genomic clone using the oligonucleotides 5′-TAAGGATCCTCTTTTCTAATTAAACCAC-3′ and 5′-ACTCGAGGTGGAGGCGAC-3′. This includes all the sequences to the next gene upstream of *MYB33*. The amplified DNA was then cloned into *Bam*HI/*Xho*I-cleaved pBluescript II SK−, and its sequence was determined to be correct. The *Bam*HI/*Xho*I fragment was then subcloned into *Bam*HI/*Sal*I-cleaved pBI 101.1, resulting in the construct p*Pro$_{33}$*:*GUS*.

For p*Pro$_{65}$*:*GUS*, the oligonucleotides 5′-TAAAGCTTGAGTCTCAAAACATAAGCCAAAAAGCCG-3′ and 5′-TAGTCGACTCTTTCTACTTAAAGCAAGACAGACTCC-3′ were used to amplify the 2145 bp immediately upstream of the ATG of the *MYB65* from Arabidopsis genomic DNA, ecotype Col. The sequences of the primers were based on the Arabidopsis BAC sequence AC008153 (which contains the *MYB65* gene). This PCR product was subcloned into *Hin*dIII/*Sal*I-cleaved pBluescript II SK−, and its sequenced was determined to be correct. This *Hin*dIII/*Sal*I fragment was then cloned into *Hin*dIII/*Sal*I-cleaved pBI 101.1, resulting in the plasmid p*Pro$_{65}$*:*GUS*.

For the p*Pro$_{33}$*:*GUS*:*3′end* construct, the 3′ end of the *MYB33* gene was amplified from the 4492-bp *Xho*I genomic clone using the primers 5′-ATGAGCTCCGAGCCCGGGAAATCCTCCACT-3′ and 5′-ATGAGCTCCTGCACGCTTTGAGATTTT-G-3′, which amplifies the 603 bp immediately downstream of the stop codon of the *MYB33* gene (Figure 5). The PCR fragment was ligated into the *Sma*I site of pBluescript II SK+, and its sequence was determined to be correct. This fragment was then cleaved out with *Sac*I and ligated into the *Sac*I site of p*Pro$_{33}$*:*GUS*. A plasmid with insert in the correct orientation was determined with a *Sma*I digest and called *pPro$_{33}$*:*GUS*:*3′end*.

For the p*MYB33*:*GUS* translational fusion, the *GUS* gene was amplified with the primers 5′-GACCATGGTATGTTACGTCCTGTAGAAACCCCA-3′ and 5′-GACCATGGTTCATTGTTTGCCTCCCTGCTGCGG-3′ from the vector pBI 101.1. The product was digested with *Nco*I and ligated into the *Nco*I site of the 4492-bp *Xho*I genomic *MYB33* clone. A clone was identified with the *GUS* gene in the correct orientation, and its sequence was determined to be correct. The *MYB33*:*GUS* gene fusion was then cleaved out with *Xho*I, and the resulting 6.3-kb fragment was subcloned into the *Sal*I site of the binary vector pPZP200-hygro (Hajdukiewicz et al., 1994), resulting in the plasmid p*MYB33*:*GUS*. Thus, *GUS* has been fused in frame to the coding region of *MYB33*, 55 amino acids from the end of the gene.

For the p*5′-MYB33*:*GUS* translational fusion, the 5′ end of the *MYB33* gene, including all upstream sequences (2044 bp upstream of the start codon), exons and introns up to amino acid 309 in the coding region (1013 bp downstream of the start codon), 10 bp before the potential miRNA target, was amplified from the 4492 bp *Xho*1 genomic clone with the primers 5′-ATGTCGACGTGGAGGCGACGTGTTCGTCAGG-3′ and 5′-TAGGATCCATATAAGGGCTTAGAATAAGGAACA-3′. This resulted in a 3071 bp amplification product, which was cloned into the *Sma* I site of pBluescript II SK+. The sequence of the amplified fragment was determined to be correct, it was then cleaved out with *Sal* I and *Bam*H1, and ligated into the *Sal* I/*Bam*H1sites of pBI 101.1, resulting in the plasmid p*5′-MYB33*:*GUS*.

For the construct p*MYB33*ΔmiR, we first amplified the 1386 bp of the 3′ end of the *MYB33* gene with the primers 5′-TAGGATCCGAAACAACATTTGACCAGTGGAAG-3′ and 5′-TAGAGCTCCTGCACGCTTTGAGATTTTGTTTTGAC-3′ and ligated the PCR fragment into the *Sma*I site of pBluescript II SK+. These sequences contain the last intron in the gene, the last 198 amino acids of the *MYB33* coding region, and 3′ sequences all the way to the gene downstream of *MYB33* (Figure 5). The fragment was sequenced and determined to be correct. The fragment was cleaved out with *Bam*HI and *Sac*I and subcloned into the *Bam*HI/*Sac*I sites of pPZP200-hygro, creating the vector pPZP200-3′end. The 5′ end fragment used in the *5′-MYB33*:*GUS* was then subcloned into the *Sal*I/*Bam*HI sites of pPZP200-3′end, resulting in the construct p*MYB33*ΔmiR.

For the constructs p*mMYB33* and p*mMYB33*-GUS, a 988-bp *Kpn*I/*Nco*I fragment containing the miR159 binding site was subcloned into pBluescript II SK+. The primers 5′-GGCAGTGAAGCTCGAATTGCCAAGCTTTCAGTATTCAGAAACAAC-3′ and 5′-GTTGTTTCTGAATACTGAAAGCTTGGCAATTCGAGCTTCACTGCC-3′ were used to introduce 10 nucleotide substitutions in the miR159 binding site, using PCR and a QuikChange site directed mutagenesis kit (Stratagene, La Jolla, CA), and this was verified by sequencing. The 988-bp *Kpn*I/*Nco*I fragment was then used to replace the corresponding sequences in p*MYB33*ΔmiR, by subcloning into the *Kpn*I/*Nco*I sites, resulting in the construct p*mMYB33*. The GUS gene was then subcloned into the *Nco*I site of p*mMYB33* to result in the plasmid p*mMYB33*-GUS.

All transgenic plants were confirmed to be carrying the correct transgene through PCR analysis and primers that were specific for each construct.

Histochemical Localization of GUS Activity

In situ GUS staining was performed using the method of Jefferson (1987). Tissues were transferred to microfuge tubes containing a solution of 100 mM Na phosphate buffer, pH 7.0, 10 mM EDTA, 0.1% Triton X-100, 2 mM potassium ferricyanide, 2 mM potassium ferrocyanide, and 1 mg/mL 5-bromo-4-chloro-3-indolyl-β-D-glucuronide at 37°C overnight or else as otherwise stated. Stained tissues were cleared with an ethanol series.

Light Microscopy

Arabidopsis inflorescences were fixed in 3% glutaraldehyde in 25 mM phosphate buffer, pH 7.2, at room temperature for several days before being rinsed in 25 mM phosphate buffer and dehydrated through a graded ethanol series. The inflorescences were then embedded in LR White resin and sliced into 1- to 2-μm transverse sections. Anther transverse sections were stained in 1% toluidine blue O and viewed under a Leica DMR compound microscope (Wetzlar, Germany) and images taken with a Leica DC200 digital camera. For examination of callose, sections were stained with 0.05% (w/v) analine blue in 0.067 M phosphate buffer, pH 8.5, and viewed under UV illumination. All GUS-stained tissues were viewed under dark-field conditions. Bright-field photographs of individual flowers or GUS-stained tissues were taken using a Wild Heerbrugg dissecting microscope and a Wild Leitz camera (Wetzlar, Germany).

ACKNOWLEDGMENTS

We thank M. Keys for technical assistance, R. King for many helpful comments and experimental suggestions, R. White and C. Miller for sectioning and microscopy of anthers, C. Davies for photography, and C. Andersson for the pPZP200-hygro binary vector. We also thank E. Dennis, B. Furbank, and R. Dolferus for critically reading the manuscript and J. Jacobsen, M. Robertson, and C. MacMillan for many useful comments. A.A.M. was funded by Graingene1, a joint venture between Australian Wheat Board Limited, the Commonwealth Scientific and Industrial Research Organization, and the Grains Research and Development Council.

Received September 27, 2004; accepted December 20, 2004.

REFERENCES

Achard, P., Herr, A., Baulcombe, D.C., and Harberd, N.P. (2004). Modulation of floral development by a gibberellin-regulated microRNA. Development **131,** 3357–3365.

Arabidopsis Genome Initiative (2000). Analysis of the genome sequence of the flowering plant *Arabidopsis thaliana*. Nature **408,** 796–815.

Campisi, L., Yang, Y., Yi, Y., Heilig, E., Herman, B., Cassista, A.J., Allen, D.W., Xiang, H., and Jack, T. (1999). Generation of enhancer trap lines in Arabidopsis and characterization of expression patterns in the inflorescence. Plant J. **17,** 699–707.

Cercós, M., Gómez-Cadenas, A., and Ho, T.-H.D. (1999). Hormonal regulation of a cysteine proteinase gene, EPB1, in barley aleurone layers: *Cis*- and *trans*-acting elements involved in the coordinated gene expression regulated by gibberellins and abscisic acid. Plant J. **19,** 107–118.

Chaudhury, A.M., Lavithis, M., Taylor, P.E., Craig, S., Singh, M.B., Signer, E.R., Knox, R.B., and Dennis, E.S. (1994). Genetic control of male fertility in *Arabidopsis thaliana*: Structural analysis of premeiotic developmental mutants. Sex. Plant Reprod. **7,** 17–28.

Chen, L., Nishizawa, T., Higashitani, A., Suge, H., Wakeui, H., Takeda, K., and Takahashi, H. (2001). A variety of wheat tolerant to deep-seeding conditions: Elongation of the first internode depends on the response to gibberellin and potassium. Plant Cell Environ. **24,** 469–476.

Chen, R., Silver, D.L., and de Bruijn, F.J. (1998). Nodule parenchyma-specific expression of the sesbania rostrata early nodulin gene SrEnod2 is mediated by its 3′ untranslated region. Plant Cell **10,** 1585–1602.

Clement, C., Chavant, L., Burrus, M., and Audran, J.C. (1994). Anther starch variations in Lilium during pollen development. Sex. Plant Reprod. **7,** 347–356.

Clough, S.J., and Bent, A.F. (1998). Floral dip: A simplified method for Agrobacterium-mediated transformation of *Arabidopsis thaliana*. Plant J. **16,** 735–743.

Diaz, I., Vicente-Carbajosa, J., Abraham, Z., Matínez, M., Moneda, I.I.-L., and Carbonero, P. (2002). The GAMYB protein from barley interacts with the DOF transcription factor BPBF and activates endosperm-specific genes during seed development. Plant J. **29,** 453–464.

Emery, J.F., Floyd, S.K., Alvarez, J., Eshed, Y., Hawker, N.P., Izhaki, A., Baum, S.F., and Bowman, J.L. (2003). Radial patterning of *Arabidopsis* shoots by class III HD-ZIP and KANADI genes. Curr. Biol. **13,** 1768–1774.

Gocal, G.F., Poole, A.T., Gubler, F., Watts, R.J., Blundell, C., and King, R.W. (1999). Long-day up-regulation of a *GAMYB* gene during *Lolium temulentum* inflorescence formation. Plant Physiol. **119,** 1271–1278.

Gocal, G.F., Sheldon, C.C., Gubler, F., Moritz, T., Bagnall, D.J., MacMillan, C.P., Li, S.F., Parish, R.W., Dennis, E.S., Weigel, D., and King, R.W. (2001). *GAMYB-like* genes, flowering, and gibberellin signaling in Arabidopsis. Plant Physiol. **127,** 1682–1693.

Goto, N., and Pharis, R.P. (1999). Role of gibberellins in the development of floral organs of the gibberellin-deficient mutant *ga1-1* of *Arabidopsis thaliana*. Can. J. Bot. **77,** 944–954.

Gubler, F., and Jacobsen, J.V. (1992). Gibberellin-responsive elements in the promoter of a barley high-pI α-amylase gene. Plant Cell **4,** 1435–1441.

Gubler, F., Kalla, R., Roberts, J.K., and Jacobsen, J.V. (1995). Gibberellin-regulated expression of a *myb* gene in barley aleurone cells: Evidence for Myb transactivation of a high-pI α-amylase gene promoter. Plant Cell **7,** 1879–1891.

Gubler, F., Raventos, D., Keys, M., Watts, R., Mundy, J., and Jacobsen, J.V. (1999). Target genes and regulatory domains of the GAMYB transcriptional activator in cereal aleurone. Plant J. **17,** 1–9.

Hajdukiewicz, P., Svab, S., and Maliga, P. (1994). The small, versatile *pPZP* family of *Agrobacterium* binary vectors for plant transformation. Plant Mol. Biol. **25,** 989–994.

Han, M.-H., Goud, S., Song, L., and Fedoroff, N. (2004). The *Arabidopsis* double-stranded RNA-binding protein HYL1 plays a role in microRNA-mediated gene regulation. Proc. Natl. Acad. Sci. USA **101,** 1093–1098.

Hurry, V.M., Strand, A., Tobiaeson, M., Gardestrom, P., and Oquist, G. (1995). Cold hardening of spring and winter wheat and rape results in differential effects on growth, carbon metabolism, and carbohydrate content. Plant Physiol. **109,** 697–706.

Ito, T., Sakai, H., and Meyerowitz, E.M. (2003). Whorl-specific expression of the *SUPERMAN* gene of *Arabidopsis* is mediated by *cis* elements in the transcribed region. Curr. Biol. **13,** 1524–1530.

Jacobsen, S.E., and Olszewski, N.E. (1991). Characterization of the arrest in anther development associated with gibberellin deficiency of the gib-1 mutant of tomato. Plant Physiol. **97,** 409–414.

Jefferson, R.A. (1987). Assaying chimeric genes in plants: The GUS gene fusion system. Plant Mol. Biol. Rep. **5,** 387–405.

Jin, H., and Martin, C. (1999). Multifunctionality and diversity within the plant *MYB*-gene family. Plant Mol. Biol. **41,** 577–585.

Kaneko, M., Inukai, Y., Ueguchi-Tanaka, M., Itoh, H., Izawa, T., Kobayashi, Y., Hattori, T., Miyao, A., Hirochika, H., Ashikari, M., and Matsuoka, M. (2004). Loss-of-function mutations of the rice *GAMYB* gene impair α-amylase expression in aleurone and flower development. Plant Cell **16,** 33–44.

Kaul, M.L.H. (1988). Male Sterility in Higher Plants. (Berlin: Springer Verlag).

Kessler, S., and Sinha, N. (2004). Shaping up: The genetic control of leaf shape. Curr. Opin. Plant Biol. **7,** 65–72.

Krysan, P.J., Young, J.C., and Sussman, M.R. (1999). T-DNA as an insertional mutagen in Arabidopsis. Plant Cell **11,** 2283–2290.

Lanahan, M.B., Ho, T.-H.D., Rogers, S.W., and Rogers, J.C. (1992). A gibberellin response complex in cereal alpha-amylase gene promoters. Plant Cell **4,** 203–211.

Larkin, J.C., Oppenheimer, D.G., Pollock, S., and Marks, M.D. (1993). Arabidopsis *GLABROUS1* gene requires downstream sequences for function. Plant Cell **5,** 1739–1748.

Lomvardas, S., and Thanos, D. (2002). Modifying gene expression programs by altering core promoter chromatin architecture. Cell **110,** 261–271.

Murray, F., Kalla, R., Jacobsen, J., and Gubler, F. (2003). A role for HvGAMYB in anther development. Plant J. **33,** 481–491.

Palatnik, J.F., Allen, E., Wu, X., Schommer, C., Schwab, R., Carrington, J.C., and Weigel, D. (2003). Control of leaf morphogenesis by microRNAs. Nature **425,** 257–263.

Park, W., Li, J., Song, R., Messing, J., and Chen, X. (2002). CARPEL FACTORY, a Dicer homolog, and HEN1, a novel protein, act in microRNA metabolism in *Arabidopsis thaliana*. Curr. Biol. **12,** 1484–1495.

Rhoades, M.W., Reinhart, B.J., Lim, L.P., Burge, C.B., Bartel, B., and Bartel, D.P. (2002). Prediction of plant microRNA targets. Cell **110,** 513–520.

Sanders, P.M., Bui, A.Q., Weterings, K., McIntire, K.N., Hsu, Y.-C., Lee, P.Y., Truong, M.T., Beals, T.P., and Goldberg, R.B. (1999). Anther developmental defects in *Arabidopsis thaliana* male-sterile mutants. Sex. Plant Reprod. **11,** 297–322.

Sorensen, A., Guerineau, F., Canales-Holzeis, C., Dickinson, H.G., and Scott, R.J. (2002). A novel extinction screen in *Arabidopsis thaliana* identifies mutant plants defective in early microsporangial development. Plant J. **29,** 581–594.

Skriver, K., Olsen, F.L., Rogers, J.C., and Mundy, J. (1991). *cis*-acting DNA elements responsive to gibberellin and its antagonist abscisic acid. Proc. Natl. Acad. Sci. USA **88,** 7266–7270.

Smyth, D.R., Bowman, J.L., and Meyerowitz, E.M. (1990). Early flower development in Arabidopsis. Plant Cell **2,** 755–767.

Stracke, R., Werber, M., and Weisshaar, B. (2001). The *R2R3-MYB* gene family in *Arabidopsis thaliana*. Curr. Opin. Plant Biol. **4,** 447–456.

Weigel, D., and Nilsson, O. (1995). A developmental switch sufficient for flower initiation in diverse plants. Nature **377,** 495–500.

Yang, S., Sweetman, J.P., Amirsadeghi, S., Barghchi, M., Huttly, A.K., Chung, W., and Twell, D. (2001). Novel anther-specific *myb* genes from tobacco as putative regulators of phenylalanine ammonia-lyase expression. Plant Physiol. **126,** 1738–1753.

The Arabidopsis *GAMYB-Like* Genes, *MYB33* and *MYB65*, Are MicroRNA-Regulated Genes That Redundantly Facilitate Anther Development

Anthony A. Millar and Frank Gubler

Plant Cell 2005;17;705-721; originally published online February 18, 2005;
DOI 10.1105/tpc.104.027920